1986 IEEE International Conference
on Robotics and Automation

Implementing a Force Strategy for Object Re-orientation

R. S. Fearing
Department of Computer Science
Stanford University
Stanford California, 94305

Abstract

This paper describes a method to reorient grasped rigid objects of polygonal cross-section using open loop force control strategies. A representation of forces in a spherical reference frame has been developed that ensures grasp stability and allows simple commands to control object reorientation. A procedure is shown for controlling at which fingers slip or rotation occurs, that can be used for three orthogonal rotations of an object grasped with three fingers. The implementation of a "twirling rotation" on the Stanford/JPL hand is described. A failure analysis is presented for potential causes for the object to slip from the grasp. Object control strategies are developed assuming line contacts and infinitesimal finger sizes. The influence of cylindrical finger tips on the performance of reorientations is described.

1.0 Introduction

Work on manipulation with dextrous hands has mostly focussed on grasping stability, achieving a good grasp, and precise control of object forces and position during small displacements (Holzmann and McCarthy, 1985; Baker, Fortune and Gross, 1985; Kobayashi, 1985; Hanafusa and Asada, 1977). Another important problem is the repositioning and regrasping of objects in a hand. Okada (1982) used finger position control to get object reorientations. This is useful during parts acquisition and assembly operations, where the easiest initial grasp to achieve is not the desired one for an assembly operation because fingers may obscure portions of object.

Unlike previous methods (Salisbury and Craig, 1982; and Cutkosky, 1984), we do not directly control the stiffness or position of the object. Instead it is proposed that for large motions, it is not practical to directly and accurately control the objects behavior using a linear mapping from finger joint behavior to object behavior. Instead object control is imposed by controlling the fingers' behavior explicitly, and imposing constraints on the object due to the applied forces that will cause its motion along desired paths. Because of the uncertainties inherent in the friction models, neither the exact time trajectory of the object, or even its exact final position will be known. This uncertainty is due to the hysteresis effect of static friction at the finger tips. For gross motions of the object with respect to the hand, slip and rolling at finger contacts is unavoidable. Therefore, it is appropriate to design control strategies that can use its effects to advantage. This was described in (Fearing 1984), and its implementation is discussed here.

Some consideration of grasping with slip and rolling contacts has recently appeared. Cutkosky (1984) examined rolling contacts and their resistance to slipping. Jameson (1985) studied grasp stability using a quasi-static analysis of combinations of sliding and fixed contacts. Kerr (1985) has analyzed the kinematics of objects rolling on finger tips without slip, which led to high order time varying nonlinear differential equations.

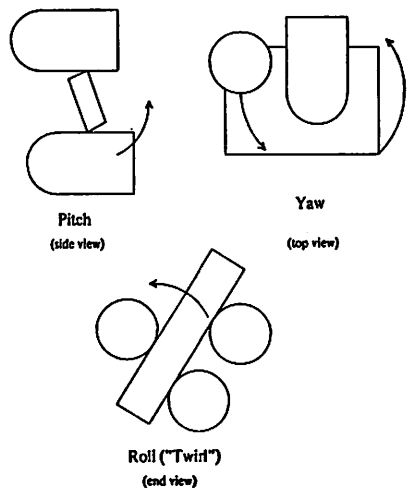

Figure 1-1. 3 Basic Object Rotations using Different Grasps

Figure 1-1 shows three basic object rotations that are reasonable for a three finger hand with only 3 degree of freedom (DOF) fingers to perform. In these 3 operations, slip and rolling are intrinsic. The sliding operations give extra equivalent degrees of freedom which are needed for hands with limited degrees of freedom. The example operation in this paper, "twirling", is a gross motion. This does not mean that fine motions can not be done with this strategy, only that accurate force control, good friction models, or contact sensing may be required to implement them.

2.0 Grasping with Disturbance Forces

For planar grasping there are only three static equilibrium equations. For this reason, a system of forces and position constraints is applied by the fingers such that there will be only three unknowns. This ensures that statically determinate analysis is possible. Assuming three finger point contacts with friction, a polar coordinate reference frame is used. It is assumed that finger forces are significantly larger than gravitational forces, so that the effect of gravity can be neglected. The three unknowns are the reaction force at a fixed position finger (finger two), and the reaction force at finger one perpendicular to the line between finger one and two. The force is specified at finger along the line between finger 1 and finger 2, and at 3, which is a "disturbance force" input to the equilibrium equations. This situation is shown in Fig. 2-1. For static equilibrium:

$$\sum_i \vec{F}_i = 0 \quad \text{and} \quad \sum_i \vec{r}_i \times \vec{F}_i = 0 \qquad (1)$$

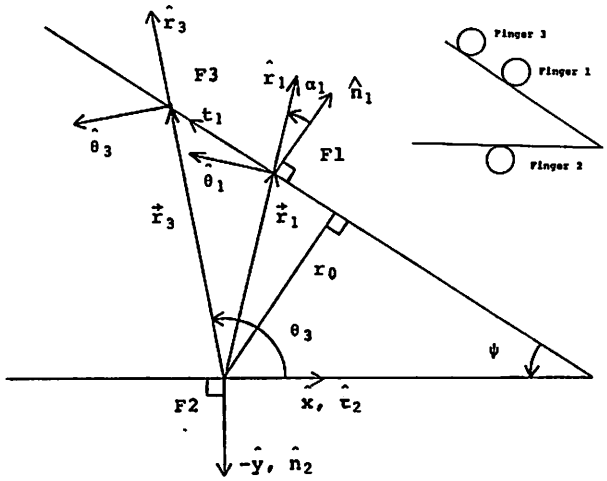

Figure 2-1. Polar Grasping Representation

where $\vec{F}_i$ are the i force vectors and $\vec{r}_i$ are the distance vectors from one point to each finger.

In addition to being statically determinate, for ease of analysis, this structure with two fingers gives moment balance and force balance automatically when finger forces are within the friction cone, that is, when ψ is less than twice the friction angle (Fearing, 1984). For two fingers, the forces are colinear, and of equal magnitude, giving equilibrium.

In polar coordinates, with respect to finger two, we have from Figure 2-1:

$$\vec{F}_1 = F_{1r}\,\hat{r}_1 + F_{1\theta}\,\hat{\theta}_1$$
$$\vec{F}_3 = F_{3r}\,\hat{r}_3 + F_{3\theta}\,\hat{\theta}_3 \qquad (2)$$

where $\vec{F}_3$ is the disturbing force applied at finger 3 (x_3, y_3), F_{1r} is the applied force, and $F_{1\theta}$ is the reaction force.

At finger two, equilibrium requires:

$$\vec{F}_2 = -(\vec{F}_1 + \vec{F}_3) \qquad (3)$$

For moment balance at finger two:

$$\vec{r}_1 \times \vec{F}_1 + \vec{r}_3 \times \vec{F}_3 = 0 \qquad (4)$$

Since the distance between the two fingers changes with the rotation, the finger one position vector is given by the geometry shown in Fig. 2-1 as:

$$\vec{r}_1 = \begin{bmatrix} x_1 \\ y_1 \end{bmatrix} = \frac{r_o}{\cos(\alpha_1 - \beta)} \begin{bmatrix} -\sin(\alpha_1+\psi) \\ \cos(\alpha_1+\psi) \end{bmatrix} = \frac{r_o\,\hat{r}_1}{\cos(\alpha_1-\beta)} \qquad (5)$$

where r_o is the normal distance from finger two to the opposite side, α_1 is the angle from from $\hat{n}_1$ and $\hat{r}_1$, and β is the rotation angle of n_2 as measured from $-\hat{y}$. The moment due to the reaction force at finger one is:

$$\vec{r}_1 \times \vec{F}_1 = |\vec{r}_1|\, F_{1\theta}\,\hat{z} \qquad (6)$$

and the moment due to the applied force at finger three is

$$\vec{r}_3 \times \vec{F}_3 = |\vec{r}_3|\, F_{3\theta}\,\hat{z} \qquad (7)$$

For moment balance:

$$F_{1\theta} = \frac{-r_3 F_{3\theta}}{r_o}\cos(\alpha_1 - \beta) \qquad (8)$$

To find the normal and tangential components of the force at finger one, the force vector is rotated by $\alpha_1' = \alpha_1 - \beta$, which is the angle from $\hat{n}_1$ to $\hat{r}_1$, to get the ratio of tangential to normal force at finger one:

$$\frac{F_{1t}}{F_{1N}} = \frac{F_{1r}\sin\alpha_1' - \frac{r_3}{r_o}F_{3\theta}\cos^2\alpha_1'}{F_{1r}\cos\alpha_1' + \frac{r_3}{r_o}F_{3\theta}\sin\alpha_1'\cos\alpha_1'} \qquad (9)$$

Now solving for equilibrium at finger 2 after transforming the force vectors at finger one into the x-y coordinate frame and rotating to get tangential and normal components at finger two, the ratio of tangential to normal force at finger two is:

$$\frac{F_{2t}}{F_{2N}} = \qquad (10)$$

$$\frac{-F_{1r}\sin(\psi-\alpha_1') - \frac{r_3}{r_o}F_{3\theta}\cos\alpha_1'\cos(\psi-\alpha_1') - F_{3r}\cos\theta_3 + F_{3\theta}\sin\theta_3}{F_{1r}\cos(\psi-\alpha_1') - \frac{r_3}{r_o}F_{3\theta}\cos\alpha_1'\sin(\psi-\alpha_1') + F_{3r}\sin\theta_3 + F_{3\theta}\sin\theta_3}$$

The reaction forces at the two fingers necessary for equilibrium have angles with respect to the surface normals defined as:

$$\alpha_1^* = \tan^{-1}\frac{F_{1t}}{F_{1N}} \quad \text{and} \quad \alpha_2^* = \tan^{-1}\frac{F_{2t}}{F_{2N}} \qquad (11)$$

The same analysis can be done when the third finger applies its force on the same side of the object as the fixed finger, finger two.

$$\frac{F_{2t}}{F_{2N}} = \qquad (12)$$

$$\frac{-F_{1r}\sin(\psi-\alpha_1') - \frac{r_3}{r_o}F_{3\theta}\cos\alpha_1'\cos(\psi-\alpha_1') + F_{3r}}{F_{1r}\cos(\psi-\alpha_1') - \frac{r_3}{r_o}F_{3\theta}\cos\alpha_1'\sin(\psi-\alpha_1') - F_{3\theta}}$$

When α_1^* and α_2^* are less than the friction angle, the object will be in equilibrium, and there will be no object motion. To get object motion, one of the force angles should be at or outside the friction cone. When one of the forces is outside the friction cone, the angles α_1^* and α_2^* are no longer defined as above, because slip occurs. Due to the constraints on object motion, the direction of slip and object rotation is known.

With slip at one of finger one or finger two, the magnitude of the translation with respect to that finger is given by:

$$\Delta s = r_o(\tan\alpha_1 - \tan\alpha_1') \qquad (13)$$

When slip occurs, the static equilibrium equations are no longer valid. However, if it is assumed that net forces on the object are small, that is dynamic forces are negligible, then a quasistatic analysis can be done. The motion of objects with pushing and force constraints using quasistatics was done for objects on a plane by Mason (1982).

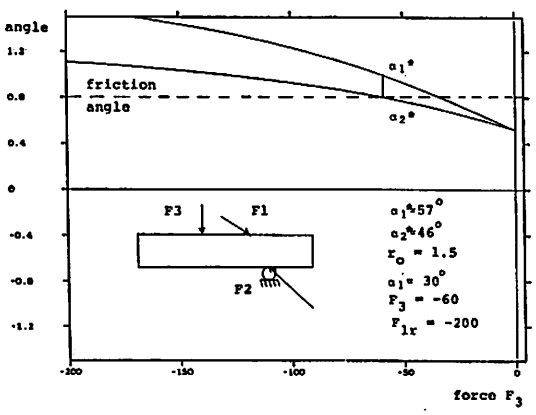

Figure 2-2. Force Angles vs. Applied Force at Finger 3

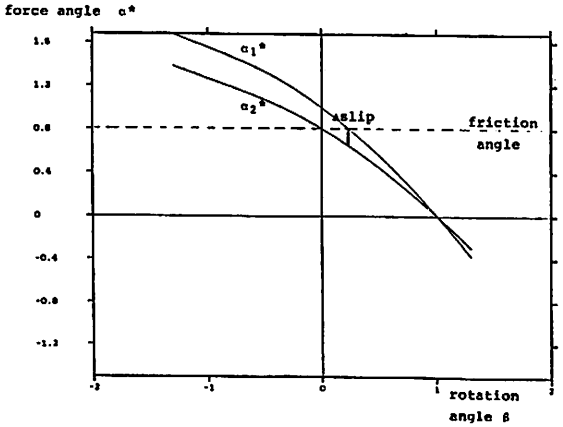

Figure 2-3. Change in Force Angles with Rotation

The force applied at finger 3 changes the force angles at fingers one and two by setting new equilibrium forces (within friction limits). This variable controls the resistance of the grasp to external disturbances, and determines the magnitude and direction of rotation. A graphical representation of Eq. 9 and 10 can be used to choose appropriate forces. Figure 2-2 shows how the force angles vary with force applied at finger three for an example of grasping a parallel edged bar. As the force at finger 3 increases from zero, the force angles at fingers 1 and 2 increase, but in this example, the force at finger one gets outside the friction cone first. With equal coefficients of friction, the first finger to slip will be on the side of the object with two fingers. With the force angle at finger one outside the friction cone, there will be a moment imbalance about finger two which will cause counter clockwise rotation about finger two with slip at finger one.

Figure 2-3 shows how the finger force angles vary as the object rotates about finger two ($\beta>0$). The object rotates until the force at the slipping finger (finger one) is again within the friction cone.

This rotation, when combined with repositioning of fingers, can be used to reorient an object. Figure 2-4 shows a sequence of repositioning of fingers and regrasping of an object for the "twirling" operation. At the start of the sequence, the object is stably grasped by three fingers. As finger one is removed from contact, the object rolls about finger 3. With finger one removed, an extra rolling motion about finger three can be applied so that finger one will not get out of its workspace when it regrabs the object. The rolling operation is discussed in detail in (Fearing, 1984). When finger one regrasps the object, the motion described by Figure 2-3 is obtained. During each cycle of this operation, the object rotates through 60 degrees.

It is important to determine if there is any net slip of the object through the fingers after a complete cycle of rotations. Such slip might lead to the object leaving the grip. The finger that slips for this sequence is always the finger with its force directed to the fixed finger. With proper positioning, the net translation should be zero after 1 full revolution of the bar, that is 6 regrasp operations. Slip magnitude is bounded during each cycle, so the part should not leave the stable grasp. Do small position errors grow? For negligible radius fingers, a displacement along the finger away from nominal position will cause a larger rotation in the next phase of regrasping, bringing the finger back to nominal position. However, unequal coefficients of friction among the fingers and positioning errors of fingers can lead to net displacement of the object.

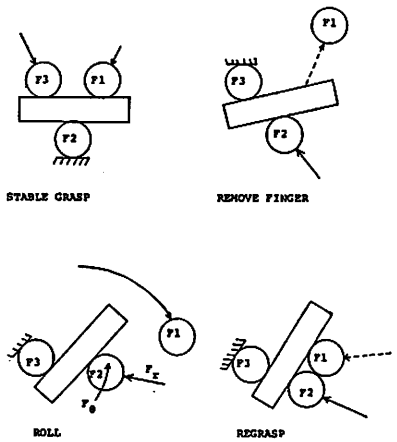

Figure 2-4. Twirling Sequence

3.0 Spherical Force Control Servo

Although the force analysis was only done for grasping in a plane, the easy extension of the same principles to three dimensional manipulation, where the desired motion is in only one plane at a time, leads to the specification of forces in spherical coordinates. For instance, by a change of orientation, twirling and the pitching motion (Figure 1-1) become equivalent operations.

Figure 3-1 shows the spherical coordinate frame. With this reference system, a finger can move at a specific distance from a point, move directly along a ray to that point, apply forces orthogonal to that ray, and other spherical operations. It is not a simple constant map from the spherical to a cartesian coordinate frame. The origin of the spherical coordinate system changes with the finger motion, and can even be attached to a moving finger if desired. This means that the transformation matrix must be updated at force servo rates. For the initial implementation, it is assumed that the dynamic forces of the fingers and object are negligible compared to the static forces.

The vector $\vec{r}$ is the displacement vector from the finger tip to the desired center of the spherical coordinate system:

$$\begin{bmatrix} r_x \\ r_y \\ r_z \end{bmatrix} = \begin{bmatrix} x \\ y \\ z \end{bmatrix} - \begin{bmatrix} x_o \\ y_o \\ z_o \end{bmatrix} \tag{14}$$

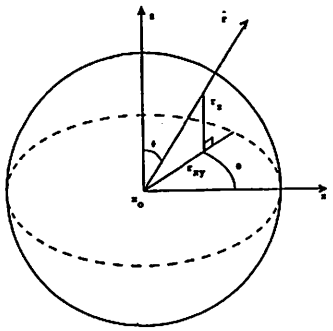

Figure 3-1. Spherical Reference Frame

The spherical error vector is:

$$\Delta\vec{r} = \begin{bmatrix} \Delta r \\ r\sin\phi\Delta\theta \\ r\Delta\phi \end{bmatrix} \tag{15}$$

$$\Delta r = |\vec{r}| - r_o \ , \ \Delta\theta = \theta - \theta_o \ , \ \Delta\phi = \phi - \phi_o$$

where $\Delta\vec{r}$ is the displacement vector, $|\vec{r}|$ is the distance of the finger from a specified origin, r_o is the nominal desired distance from that origin, and $\Delta\theta$ and $\Delta\phi$ are the angle differences from the desired orientation.

Using a diagonal stiffness matrix in spherical space, the desired force in spherical space is determined from:

$$\vec{F}_r = \vec{F}_o + \begin{bmatrix} k_r & 0 & 0 \\ 0 & k_\theta & 0 \\ 0 & 0 & k_\phi \end{bmatrix} \Delta\vec{r} \tag{16}$$

where $\vec{F}_o$ is a constant bias force, and k_r, k_θ, and k_ϕ are stiffness terms. The angles of interest are obtained from:

$$r = \sqrt{r_x^2 + r_y^2 + r_z^2} \ , \ r_{xy} = \sqrt{r_x^2 + r_y^2}$$

$$\phi = \tan^{-1}\frac{r_{xy}}{r_z} \ , \ \theta = \tan^{-1}\frac{r_y}{r_x} \tag{17}$$

The transformation matrix from spherical to cartesian coordinates is given by:

$$\mathbf{K}_s = \begin{bmatrix} \sin\phi\cos\theta & -\sin\theta & \cos\theta\cos\phi \\ \sin\phi\sin\theta & \cos\theta & \sin\theta\cos\phi \\ \cos\phi & 0.0 & -\sin\phi \end{bmatrix} \tag{18}$$

To convert the desired force from spherical to cartesian coordinates:

$$\vec{F}_s = \begin{bmatrix} F_x \\ F_y \\ F_z \end{bmatrix} = \mathbf{K}_s \begin{bmatrix} F_r \\ F_\theta \\ F_\phi \end{bmatrix} - k_v \begin{bmatrix} \dot{x} \\ \dot{y} \\ \dot{z} \end{bmatrix} \tag{19}$$

where k_v is a velocity damping factor for stability. The desired finger joint torques are had from:

$$\vec{\tau} = \mathbf{J}^T(\theta)\,\vec{F}_s \tag{20}$$

where J is the Jacobian matrix for the finger, and $\vec{\tau}$ is the vector of finger joint torques.

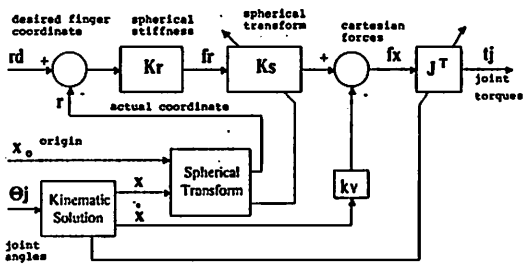

Figure 3-2. Spherical Servo Block Diagram

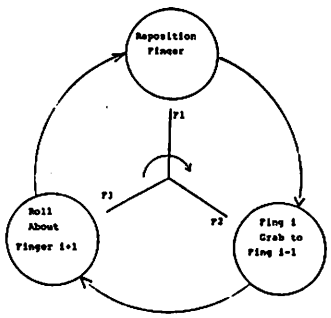

Figure 3-3. Twirling Gait

Figure 3-2 shows the overall structure of the spherical control servo. In the implementation on a PDP-11/60, the spherical servo executes at 33 Hz for all three fingers of the Stanford/JPL hand.

The joint torque control servo uses a simple proportional-derivative tendon tension controller for each tendon. This simple scheme ignores the dynamics of the coupling between the tendons, and so reduces the obtainable finger frequency response. This structure was adapted from Salisbury and Craig (1982). Tendon tension gain is set high to minimize the effects of motor stiction. This servo level runs at 100 Hz on the 11/60. There is no available proof that servos should be run at different rates, but empirically, improved stability is observed with higher servo rates.

Implementation

To achieve adequate grasp stability when only two fingers are contacting the object, as when a finger is being repositioned, line contacts with friction were required. Each line contact has 5 contact wrenches, which give more than the 7 required for complete restraint of the object (Lakshminarayana, 1978). The compliance of the fingertips also improves the contact area to get a larger friction coefficient (Fearing, 1983). With a 3 DOF finger, only the location of a point in space can be specified, not the line orientation and location. A grasp configuration was chosen that allows line contacts in the small plane of operation. With only 3 DOF in each finger, slip is really needed to achieve object mobility.

A consecutive plan of forces and finger motions is applied using the spherical force servo. The analysis of Section 2 was used to develop a strategy of forces that will cause object rotation and slip at the desired fingers. A table of 3 finger operations (Figure 3-3) determines the order of operations for each finger. Using this "twirling gait" the object rotates through 180 degrees for every complete cycle of 3 operations. With smooth transitions between phases, there are only three operations: bringing a finger around to the other side of the object, applying a force directed towards the next lower number finger, and rolling about the next higher number finger. The rolling operation is described in more detail in (Fearing, 1984).

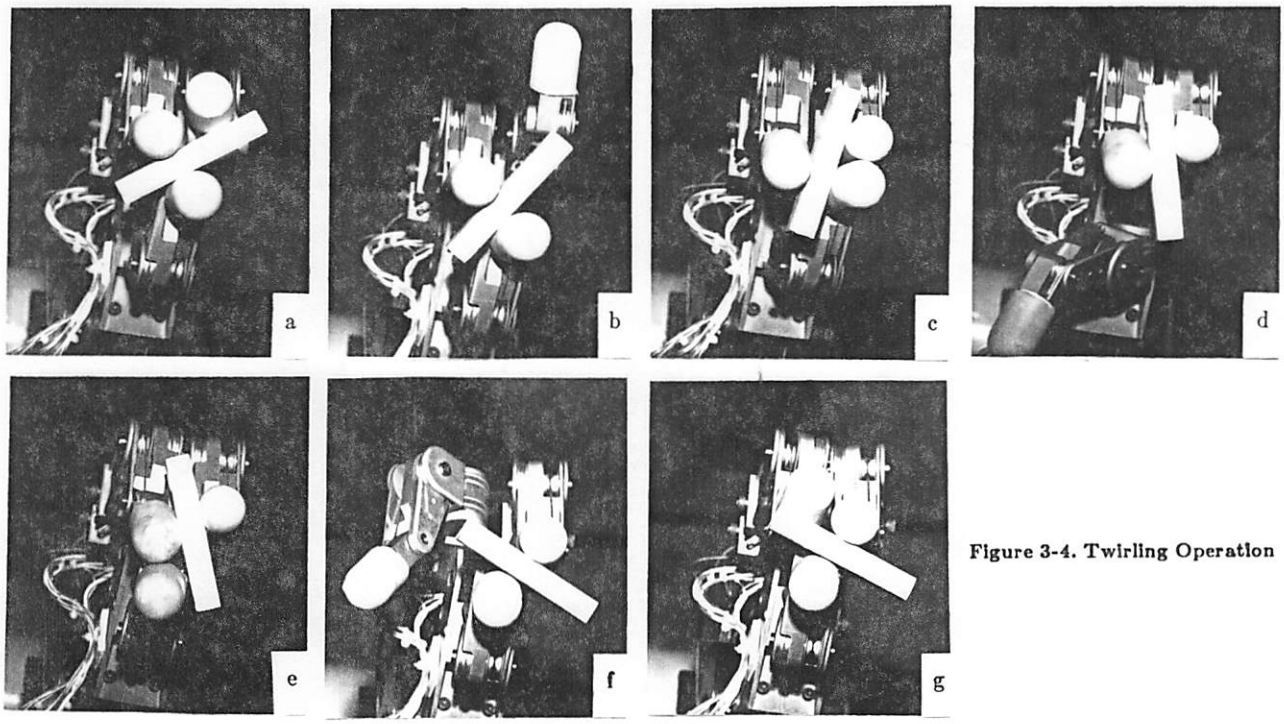

Figure 3-4. Twirling Operation

Fig. 3-4 shows experimental results for twirling an aluminum bar from a single run. Operational speed is about 8 seconds per regrasp operation, and is limited mainly by instability at the tendon servo level. Typical performance is about 3 half revolutions of the bar before it becomes displaced sufficiently for the next grasp operation to fail. Common failure modes with the bar are a yawing motion out of the twirling plane, and translation of the bar so that it collides with the finger at an inappropriate location, which can force the object out of the grasp. Tactile sensing is useful for more robust operation.

4.0 Force Errors with Contact Location

When using open loop force strategies to control object motion, it is important to consider the sources and effects of errors in applied forces at the finger contacts. Salisbury and Craig (1982) considered the effect of errors in joint space on the fingertip force space, using the condition number of the Jacobian. Cutkosky (1984) considered small errors in contact location and the effect on actual applied forces, and used the differential Jacobian matrix which keeps the analysis linear. Yoshikawa (1984) developed a manipulability measure that considers the ability of a mechanism to move and exert forces in various directions for given joint configurations and link lengths.

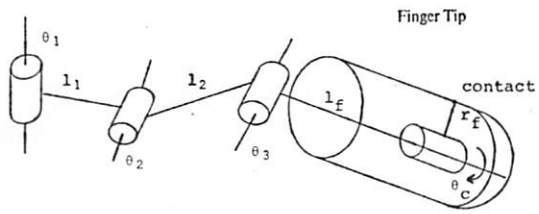

Figure 4-1. Finger Kinematics

The force analysis of Section 2.0, and the servo implementation of Section 3.0 assume that the object contacts the finger at a point, and that this location is fixed on the finger. Figure 4-1 shows the actual finger kinematics when a cylindrical finger tip is used on the finger of the Stanford/JPL hand. The complete kinematics for a given contact location can be derived that depends on the finger radius r_f, and two changing parameters, l_f the finger tip length to the contact, and θ_c, the angle about the finger at which contact is made. For speed considerations, and due to the lack of finger contact sensors, the servo implementation assumes that $r_f = 0$ and that l_f is constant, 5 cm, about 1 cm less than the length to the tip.

Since no contact sensors are used with the present force servo scheme, and the object can roll anywhere about the cylindrical fingertip, the actual contact location may be at any θ_c, and displaced several cm. from directly beneath the finger center. These are the typical errors that can be expected. (Constraints from the finger tip locations in space could be used to determine the attitude and position of the object with respect to each finger, but this has not been attempted).

Here a measure of the sensitivity of the desired forces to the contact location is developed. The desired joint torques for an assumed contact are determined from the Jacobian matrix, and then the actual forces are predicted for various contact locations (assuming fixed point contacts with no slip). The desired joint torques are calculated from the desired cartesian finger tip forces:

$$\vec{\tau}_j = \mathbf{J}^T(\theta)\,\vec{F}_s \tag{21}$$

The actual force applied at a particular contact location can be found by using the inverse Jacobian that considers the more complete finger model:

$$\vec{F}_a = \mathbf{J}'^{-T}(\theta_a)\,\mathbf{J}^T(\theta_d)\,\vec{F}_d \tag{22}$$

where $\mathbf{J}'$ is the Jacobian matrix for the changed contact geometry; $\mathbf{J}$ is the Jacobian when the finger has negligible radius, and the contact always occurs at a fixed distance along the finger; and $\vec{F}_d$ is the desired force vector for the assumed contact.

As an example, the resultant forces were calculated for the finger of the Stanford/JPL hand in the pose used to obtain line contact with the object in the "twirling" operation. Figure 4-2 shows how the direction of the actual force changes along the bottom of the finger for a desired force in the $\hat{y}$ direction, where each line on the finger represents the resultant force if the contact were at that location. Several interesting properties of the change in forces are apparent. One is that the pattern of force vectors can be either divergent or convergent, depending on the finger posture. For the divergent case, a displacement of the grasped object's contact point from directly under the calculated contact location results in an increased tangential component to the force directed away from the expected location. This increased tangential component may result in a further tendency for horizontal displacement, so this is an unstable contact condition. This shows the importance of using contact sensors to determine and correct for the object contact location. For the convergent case, which occurs with the fingers closer together, a contact error will tend to have a restoring force error back to the nominal position.

When rolling the bar between the cylindrical finger tips, depending on which edge of the bar contacts the finger, a net moment about the axis between the two opposing fingers can develop. This can lead to greater position errors, and dropping of the object.

An interesting property shown by this analysis is that because of the width of the finger tip, there is a singularity of the mechanism along the finger tip. For reasonable force control, this location and all locations along the finger towards its base end should be avoided.

The other position error is due to the object rolling around the main axis of the finger θ_c. As Figure 4-3 indicates, here the force direction remains basically the same, and the magnitude increases towards the base of the finger. (This is as expected, for constant torque at the third joint, a shorter moment arm can apply more force).

So for a round finger, the force may be offset from the desired location, yet still have approximately the same direction and magnitude. Cutkosky (1984) has analyzed the forces with finger tips rolling on the object. Figure 4-4 shows how the approximation of negligible finger radius does not adversely effect the grasping and manipulation strategies developed in Section 2.0. The force location is offset by the finger radius, so in general, there will be moment due to the force vectors not being colinear. However, this moment will tend to rotate the object so that the finger forces become more colinear.

Cutkosky (1984) showed how certain grasp configurations can be made unstable by increasing finger forces without increasing finger stiffnesses. The analysis here indicates another source of instability due to the uncertainty in contact location which is dependent on finger configuration.

Section 5.0 Conclusion

A force strategy for the full rotation of an object in a plane with three fingers was developed using a point contact with friction model. The force strategy is robust with respect to object size and shape. A spherical servo system was developed that can use this strategy, and can be used for other reorientation operations. An experimental trial was shown on the Stanford/JPL hand. Limits to open-loop force strategies were found due to changing forces with contact location on a cylindrical finger tip.

For more certain operation, finger tip contact sensing would be very helpful. Yet the open loop force strategies for manipulation are useful for finding the minimum requirements of contact sensors, and for providing a standard of comparison for the enhancement provided by finger tip tactile sensors.

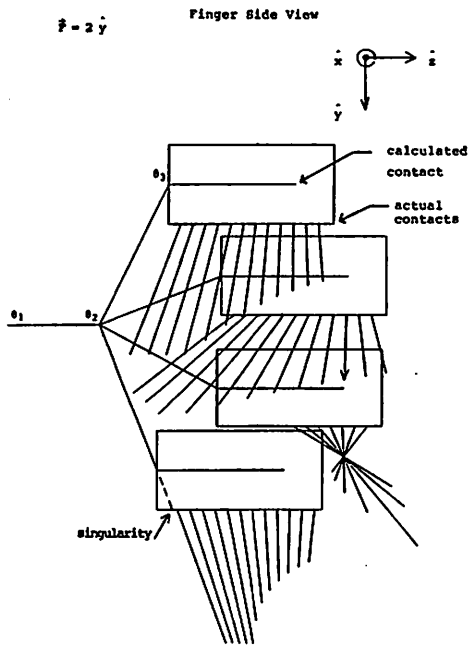

Figure 4-2. Force Errors along Finger Length

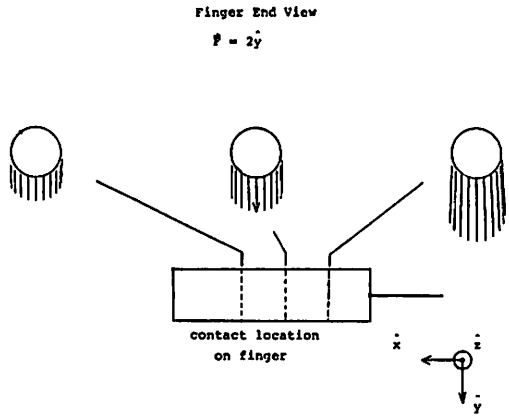

Figure 4-3. Force Errors around Finger Circumference

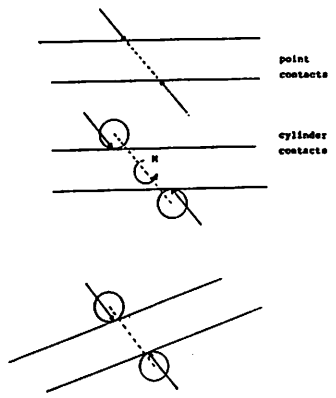

Figure 4-4. Grasping with Cylindrical Fingertips

Acknowledgement

Support for this research was provided by DARPA contract F33615-82K-5108. Thanks to Joel Burdick and Dave Kriegman for helpful discussions on force control and representation systems. Thanks to Tom Binford for his suggestions on finger gaits and for his encouragement of experimental verification of theory.

REFERENCES

[1] B.S. Baker, S. Fortune, E. Grosse, "Stable Prehension with a Multi-Fingered Hand', Proc. IEEE Conf. on Robotics and Automation, St. Louis, Missouri, March, 1985.

[2] M.R. Cutkosky, "Mechanical Properties for the Grasp of a Robotic Hand", CMU Robotics Institute Tech. Report CMU-RI-TR-84-24, 1984.

[3] R.S. Fearing, "Simplified Grasping and Manipulation with Dextrous Robot Hands", Proceedings, American Control Conference, San Diego, CA, June 1984.

[4] R.S. Fearing, "Touch Processing for Determining a Stable Grasp", S.M. Thesis, MIT EE&CS, Sept. 1983.

[5] H. Hanafusa and H. Asada, "Stable Prehension by a Robot Hand With Elastic Fingers," *7th ISIR,* Oct. 1977.

[6] W. Holzman and J.M. McCarthy, "Computing the Friction Forces Associated with a Three Fingered Grasp", Proc. IEEE Conf. on Robotics and Automation, St. Louis, Missouri, March, 1985.

[7] J.W. Jameson, "Analytic Techniques for Automated Grasping ", Ph.D. Thesis, Dept. of Mechanical Engineering, Stanford University, 1985.

[8] J.R. Kerr, "An Analysis of Multi-Fingered Hands", Ph.D. Thesis, Dept. of Mechanical Engineering, Stanford University, 1985.

[9] H. Kobayashi, "Control and Geometrical Considerations for an Articulated Robot Hand," *International Journal of Robotics Research,* Vol. 4, No. 1, Spring 1985.

[10] M.T. Mason, "Manipulator Grasping and Pushing Operations," MIT AI Lab AI-TR-690, June 1982.

[11] T. Okada, "Computer Control of Multijointed Finger System for Precise Object-Handling," *IEEE Transactions on Systems, Man, and Cybernetics,* Vol. SMC-12, No. 3, May/June 1982.

[12] J.K. Salisbury and J.J. Craig, "Articulated Hands: Force Control and Kinematic Issues," *International Journal of Robotics Research,* Vol. 1, No. 1, Spring 1982.

[13] T. Yoshikawa, "Manipulability of Robotics Mechanisms", Second International Symposium of Robotics Research, Tokyo, Japan, August 20-23, 1984.